energies

Article

Integration of Traction Electricity Consumption Determinants with Route Geometry and Vehicle Characteristics

Arkadiusz Kampczyk [1,*], Wojciech Gamon [2] and Katarzyna Gawlak [2]

[1] Department of Engineering Surveying and Civil Engineering, Faculty of Geo-Data Science, Geodesy, and Environmental Engineering, AGH University of Science and Technology, al. A. Mickiewicza 30, 30-059 Krakow, Poland
[2] Department of Railway Transport, Faculty of Transport and Aviation Engineering, Silesian University of Technology, ul. Krasińskiego 8, 40-019 Katowice, Poland
* Correspondence: kampczyk@agh.edu.pl

Abstract: Traction electricity (TE) consumption in rail transportation (rail transport) is determined by factors (determinant) related to the characteristics of railway lines and vehicles. They have an impact on driving speeds, which, in turn, affect energy consumption. The scientific research presented here combined the results of expert, direct and indirect measurement methods, including brainstorming, mind mapping, system approach, heuristics, failure mode and effect analysis. The main objective was to demonstrate the influence of the determinants of TE consumption, depending on the route (road) geometry and characteristics of the traction of electric vehicles and whole trains (catenary-supplied electric vehicles, non-autonomous electric vehicles, and network traction vehicles, especially electric locomotives and electric multiple units, electric multiple-units (EMUs)). Using a new approach, the TE consumption equation, we applied values for the movement resistances of electric locomotives during braking for a jointed railway track $M_{res\ JRT\ braking}$ and continuous welded rail tracks $M_{res\ CWRt\ braking}$. The values of the movement resistances of the electric locomotives during startup on the jointed railway track $M_{res\ JRT\ startup}$ and continuous welded rail tracks $M_{res\ CWRt\ startup}$ were also applied. They showed a strong correlation with the existing speeds of catenary-supplied electric vehicles. The implementation of the new innovative approach is an important contribution to the development of engineering and technical sciences, in particular, the disciplines of civil engineering, surveying/geodesy, and transport.

Keywords: traction; catenary; electrified traction system; electric traction; traction drive; sustainability development; jointed railway track (JRT); continuous welded rail track (CWR track); monitoring; movement resistances; energy consumption; startup; braking; geometry

check for updates

Citation: Kampczyk, A.; Gamon, W.; Gawlak, K. Integration of Traction Electricity Consumption Determinants with Route Geometry and Vehicle Characteristics. *Energies* **2023**, *16*, 2689. https://doi.org/10.3390/en16062689

Academic Editor: Salman Mohagheghi

Received: 3 February 2023
Revised: 6 March 2023
Accepted: 8 March 2023
Published: 13 March 2023

Copyright: © 2023 by the authors. Licensee MDPI, Basel, Switzerland. This article is an open access article distributed under the terms and conditions of the Creative Commons Attribution (CC BY) license (https://creativecommons.org/licenses/by/4.0/).

1. Introduction

The efficiency of rail transport (rail transportation) is one of the most important pillars of sustainability development systems (SDS). Therefore, the integration of traction electricity (TE) consumption determinants (factor) with the characteristics of route (road) geometry and electric traction vehicles and whole trains (catenary-supplied electric vehicles, non-autonomous electric vehicles, and network traction vehicles, especially electric locomotives and electric multiple units, electric multiple-units (EMU)) is crucial. At the same time, rail transport is one of the most important sectors of the economy, contributing to economic growth. The monitoring of and the correlation between the energy consumption of electric vehicles, their speeds and traffic data, and the geometry of roads was addressed by Morlock et al. [1], Yan et al. [2], Ferreir et al. [3], Karwowski et al. [4], Haładyn [5], and Song et al. [6]. The consumption of traction electricity in rail transport is determined by the factors characterizing the railway lines and the catenary-supplied electric vehicles. These factors have an impact on the vehicles' driving speeds, on which energy consumption depends. Catenary-supplied electric vehicles are vehicles to which electricity is supplied via the catenary (the overhead contact line). Energy consumption depends on a number of determinants, mainly reflected in the management of traction power supply systems. The problems shaping the subject of factors influencing energy consumption have been addressed in numerous publications [7–19].

Attention has been drawn to the electromechanical simulation of traction systems by Boschetti and Mariscotti [7], who stated that both analysis and electromechanical simulation are required to conduct energy consumption assessments, while Zalewski [8] emphasized that the influence of atmospheric factors is significant. Among the climatic factors, Zalewski specifically identified air temperature, humidity, wind strength, rainfall, pressure, and sunshine, referring to an analysis of the effects of ambient temperature and day length on electricity consumption at four selected transformer stations supplying a single-family housing estate, blocks of flats, a retail and service pavilion, and a city market [8]. Zalewski [8] found that the value of the ambient temperature and the length of the day significantly impact electricity consumption. Thus, the consumption depends on the consumer and the time of year. Douglas et al. [9] pointed to the dependence on the route, vehicle, and service characteristics. At the same time, however, they emphasize that there is little information in the literature on which solutions are most suitable for each type of network and how they interact with each other. Su et al. [10] referred to the state of traction energy consumption in metro systems by analyzing the influence of factors in the optimal train control model on traction energy consumption using the optimal train control simulator (OTCS). In turn, Lin et al. [11] addressed the speed prediction using the Markov chain model combined with a driving pattern recognition application to evaluate the energy consumption of a dual-motor electric vehicle. Ćwil et al. [12] focused on the problem of railway vehicles' energy efficiency in relation to sustainable transportation systems. The authors made particular reference to methods of measuring energy consumption in the railway transportation sector and the inclusion of energy consumption as a criterion for railway tenders' rolling stock. At the same time, Ahmed et al. [13] developed an integrated optimization model to simultaneously optimize the station locations and the line network connecting them, using a geographic information system (GIS) and a genetic algorithm (GA). Fischer and Szürke [14] highlighted the cost-effective trend in rail transport towards regenerative braking energy. In their illuminating study, the authors showed that the value of regenerative braking energy could be as high as 20–30% of the total energy used. They emphasized that this unused energy can be used, for instance, to address the comfort demand for air conditioning, heating, lighting, etc., or in energy-intensive startups (energy-intensive starts). Fischer [15] drew attention to speed limits, which cause a significant increase in traction energy consumption, while Naldini et al. [16] focused on the solutions to (a) the real-time rail traffic management problem (rtRTMP), and (b) the real-time energy consumption minimization problem (rtECMP). Their objective 'is to minimize the weighted sum of train energy consumption and total delay'. Using the self-organizing data mining method, Ren et al. [17] argued that traction energy accounts for the majority of energy consumed by electric multiple-unit trains. At the same time, Jefimowski [18] recognized that factors could be broadly divided into those arising from the performance of the railway line and those arising from the performance of the railway rolling stock, and both groups affect the train speed. Spiryagin et al. [19] highlight problems, assumptions, and solutions in locomotive design, traction, and operational studies, particularly emphasizing the importance of systems engineering, which depends on knowledge from many disciplines.

Currently, along with the studies on well-known applications of modelling and energy consumption [20–25], research is also being carried out on eco-driving, i.e., economical driving, which determines the fastest possible route while maintaining safety and saving energy and the environment [26–30], on renewable energy [31–33], optimizing timetables [34–39], traction system monitoring [40,41], inverters (falownik in Polish) [42–45], and the dynamics of vehicle movement [46–53].

Integration of traction electricity consumption determinants in correlation with route geometry and vehicle characteristics constitutes an interconnected system in which one element impacts the other. Thus, Gonzalez et al. [54] referred to mobility maps for ground vehicle route planning, while Zhong et al. [55] focused on the online generation of train speed profiles with energy saving. In contrast, Bin et al. [56] referred to neutral sections in optimizing the energy-efficient speed profiles (ESPs). Heirich et al. [57] presented simultaneous localization and mapping relying exclusively on train-side sensors, known as RailSLAM, and localization of rail vehicles and mapping of geometric railway tracks. Lei and Noda [58] examined the irregularities in conditions of the track vertical profile.

The impulse motivating this study is guided by the research carried out by Burak-Romanowski and Woźniak [59], Kacprzak [60], and Biliński et al. [61]. Burak-Romanowski and Woźniak [59] presented the basic principles of electric traction or traction electricity: properties, resistance to vehicle movement, and consumption of traction electricity. They referred to the increase in the smoothness of driving traction vehicles as the amount of electricity they consume. They analyzed the amount of energy consumption as a function (depending) of the speed of individual types of railway rolling stocks and their weight. They considered the actual profiles of the railway lines and a didactic information technology (IT) tool. The authors of this paper have identified the existing approach outlined in [59] as Variant I. In turn, Kacprzak [60] took up the theory of electric traction, and Biliński et al. [61] referred to the resistance of traction vehicle movement with empirical equations, presenting and systematizing existing relationships. They found this approach helpful 'in engineering calculations of estimated energy consumption'. They emphasized 'the need to verify the results of the simulation with the results obtained under conditions of actual operation' [61].

Thus, the main objective of this study is to demonstrate the influence of TE consumption determinants, depending on the route geometry and characteristics of the electric traction vehicles and whole trains, using a new approach that applies the movement resistance values of electric locomotives during braking on jointed railway tracks $M_{res\ JRT\ braking}$ and continuous welded rail tracks $M_{res\ CWRt\ braking}$, and the values of the movement resistance of electric locomotives during startup (starting) on jointed railway tracks $M_{res\ JRT\ startup}$ and continuous welded rail tracks $M_{res\ CWRt\ startup}$. With this new approach, named Variant II (following Variant I developed by [59]), we used the TE consumption equation to monitor electric energy consumption q_i, including total specific energy consumption during breaking measured at the motor terminals j_i for a jointed railway track (JRT) and a continuous welded rail track (CWRt, CWR track) in correspondence with [62] and during startup for JRT and CWRt.

The results of our research were compared with the results obtained under the real exploitation conditions of EMUs—data from the recorders of the individual electric traction vehicles and the state of the railway superstructure (permanent way, permanent track and railway surface). The results were also correlated with summer and winter seasonal data. They show a strong correlation with the existing speeds of railway catenary-supplied electric vehicles. The implementation of this new innovative approach is an important contribution to the development of engineering and technical sciences, in particular, the disciplines of civil engineering, surveying/geodesy, and transport.

To date, no attempt has been made to monitor electric energy consumption q_i, including total specific energy consumption measured for JRT and CWRt at the motor terminals j_i during breaking and startup together with the results obtained from real exploitation conditions, both from the EMU recorders and the state of the railway superstructure. A review of the relevant literature revealed a lack of research using the approaches proposed in this study. The research topic pursued here fits the scope of the examined literature and attempts to fill the existing gap within its field of study, following the work presented in [62,63]. Kampczyk [62] undertook research on determinants of specific traction electricity consumption in an SDS rail transport, presenting the monitoring equations of electric energy consumption q_i during braking on both jointed railway track and continuous welded rail tracks.

A clear correlation was found in [62] among many determinants of unit traction electricity consumption in SDS rail transport [62]. Subsequently, in [63], reference was made to energy consumption by catenary-supplied electric vehicles of the series EN57AKŚ with particular emphasis on their thermal insulation, and thus the energy loss associated with the need to heat the passenger area. The authors of [63] presented the results of their research carried out on selected types of EMUs with a specific focus on regional transport. The authors found, among other things, inadequacies in the thermal insulation of the vehicle series EN57AKŚ, such as insufficient insulation of the front door seals and a significant heat loss due to the construction of the railway car interconnections (so-called folding connections or interunit connections)—areas joining two adjacent sections of the vehicle [63]. In this study, the authors present the elements of the research developed following [62,63].

The results of the research carried out support the international forum of researchers. They crystallize the realized and implemented results of the development in the field of engineering and technical sciences and the industry, especially for decision and policy makers to further improve the monitoring of traction energy consumption in correlation with the route geometry and characteristics of traction electric vehicles and whole trains. They impact the improvement of a sustainability and ecological railway system while representing an important global scientific research task as a leading trend for effective monitoring.

The new approach presented in this publication leads to an increase in the integration of traction electricity consumption determinants in correlation with route geometry and vehicle characteristics.

Nevertheless, the requirements for scientific research into both route geometry and vehicle characteristics are complex and time consuming, relying on expertise and numerous instruments, and the integration of direct measurement methods (DMM), indirect measurement methods (IMM), and expert methods (EM) with brainstorming (BM), mind mapping (MMM), system approach (SAM), heuristic (HM), and failure mode and effect analysis (FMEA) methods. The challenge was to take a step forward, and the authors of this publication—an interuniversity scientific research team—responded with an industry-based practice that ensures seamless integration of data, including data of different physical sizes, and the possibility of implementing new approaches, such as Variant II. At the same time, the research subject advanced the integration of traction electricity consumption determinants with route geometry and vehicle characteristics for effective monitoring and diagnostics. The article was prepared under the scientific research subvention of AGH University of Science and Technology No. 16.16.150.545 in 2023.

2. Materials and Methods

2.1. Route Geometry Architecture: Railway Lines

This study covered the complete route from Lubliniec station to Katowice station, located in the Silesian Voivodship in Poland, with a length of 62.741 km (Figures 1 and 2). A total of 17 numbered points representing the stations and passenger stops on the railway lines are represented in Figure 1. The names of the stations and passenger stops in the plane are shown in Figure 1a corresponding to the cartographic development background [64], and the elevation–longitudinal profile, is presented in Figure 1b.

The complete route includes segments of three railway lines:

- No. 143 from Lubliniec station to Kalety station (first-rate railway line category, first-class railway line category);
- No. 131 from Kalety station to Chorzów Batory station (magistral railway line category, main railway line category);
- No. 137 from Chorzów Batory station to Katowice station (magistral railway line category).

A railway superstructure is a structural assembly comprising the following, among others:

- Rails;
- Sleepers;
- Ballast;
- Rail fastening elements.

(**a**)

(**b**)

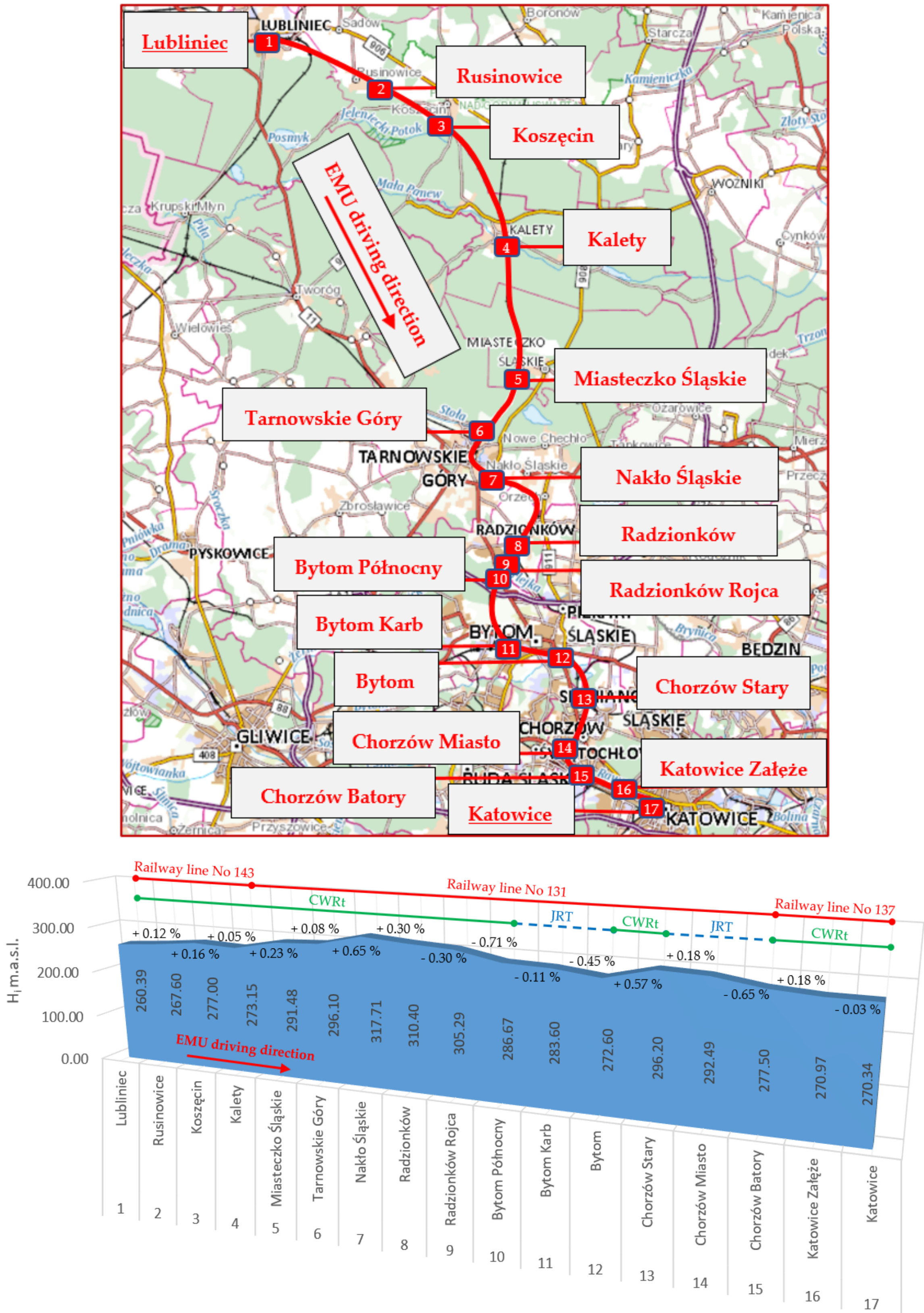

Figure 1. Exposure of route geometry in the plane: (**a**) situational; (**b**) elevation–longitudinal profile, length of 62.741 km, where: 1–17 are passenger stops or stations; EMU—electric multiple unit; H_i—elevation coordinate expressed in the state spatial reference system in [m.a.s.l.]; CWRt—continuous welded rail track; JRT—jointed railway track.

(**a**)  (**b**) 

Figure 2. Railway infrastructure between (**a**) points 1 Lubliniec and 2 Rusinowice, and (**b**) points 3 Koszęcin and 4 Kalety.

It is adapted to carry rail vehicle loads on the subgrade (Figure 2). The subgrade as a geotechnical structure represented by embankments (fill) and cuttings, including safety and drainage facilities. The technical and exploitation characteristics of the route segments, classified as first-rate and magistral railway lines, are included in Table 1 and comply with legal regulations [65–70], taking into account international law. The complete route, including the three railway lines, is an electrified railway line in the 3 kV direct current (DC) electric traction system.

Table 1. Technical exploitation specifications of the complete route.

Technical Exploitation Parameters of Railway Lines		
Name	**First-Rate**	**Magistral**
exploitation load T	$10 \leq T < 25$	$T \geq 25$
speed of passenger trains V_m	$80 < V_m \leq 120$	$120 < V_m \leq 200$
speed of freight trains V_{tow}	$60 < V_{tow} \leq 80$	$80 < V_{tow} \leq 120$
permissible axle loads P	$210 \leq P < 221$	$P \leq 221$

where T is Tg/year; V_m is km/h; V_{tow} is km/h; P is kN.

Figure 1 shows the maximum difference in elevation (h_{mi}) of structural objects along the complete route between the following:

- The start of the route at point 1 Lubliniec, to point 7 Nakło Śląskie, with an elevation of h_{m1} = 57.32 m; the value of the slope angle in this segment is α_1 = +0.16 %;
- Point 7 Nakło Śląskie, and 17 Katowice – the endpoint of the route with the elevation of h_{m2} = 47.37 m; the value of the slope angle in this segment is $\alpha_2 = -0.18$ %.

The complete Lubliniec–Katowice route constructed railway is represented as a linear object constituting the base in our research, and following [71–75], it is qualified as plain, flat terrain. Figure 1 illustrates the configuration of the route geometry in the plane (situational) (Figure 1a) and elevation (longitudinal) profiles (Figure 1b). For each of the 16 constituent segments of the complete route, slopes are characterized in percentage terms (Figure 1b). The elevation coordinates H_i measured in m.a.s.l. are expressed in the national elevation system for each individual component point 1–17 of the complete route [76–79] (Figure 1b). The linear object representing the complete route includes jointed railway tracks and continuous welded rail tracks. The railway track is the fundamental load-bearing system of the railway superstructure, the geometrical arrangement of which is calibrated for the safe movement (traffic) of railway vehicles at speeds and pressures (loads) defined by technical and exploitation parameters [65,70]. A jointed railway track is a railway track with standard-length rails joined by rail fishplates or with welded rails of lengths greater than the standard but less than 180 m. A continuous welded rail track is a railway track with welded rails 180 m and more in length [65,70]. Both types of tracks cover segments of the Lubliniec–Katowice line in the following sequence (Figure 1b):

- 1–10: Lubliniec–Bytom Północny–CWRt;
- 10–12: Bytom Północy–Bytom–JRT;
- 12–13: Bytom–Chorzów Stary–CWRt;
- 13–15: Chorzów Stary–Chorzów Batory–JRT;
- 15–17: Chorzów Batory–Katowice–CWRt.

2.2. Characteristics of Traction Electric Vehicle: Electric Multiple Units

The study was carried out using two catenary-supplied electric vehicles of the series EN57AKŚ (EN57AKŚ-223 and EN57AKŚ-730) (Figure 3), which are three-car electric multiple units designed for local traffic.

(**a**) 

(**b**) 
(**c**) 

Figure 3. Electric multiple unit of the EN57AKŚ-223 series: (**a**) front end with the whole vehicle visible; (**b**) passenger compartment; (**c**) passenger and bicycle compartment.

They consist of three permanently connected two-bogie, four-axle railway cars/wagons (it is possible to disconnect the unit under workshop conditions). The two end carriages are the control carriages containing the drivers' cabins, while the middle is the driving carriage (motor bogie) where all four of its engines are installed.

The EN57AKŚ vehicles are based on the construction of the classic EN57 vehicle used in Poland and other countries (e.g., Slovenia and Croatia) since the 1960s. The EN57AKŚ vehicle is a modernized version of a classic vehicle, in which several changes and improvements have been made, including replacing DC series motors with asynchronous motors. During the upgrade, many other modifications were made, such as replacing the dynamic inverter with a more modern static inverter, installing a fast circuit breaker, and adding an electronic speedometer to record driving parameters. One of the most important modifications was the addition of an electricity meter placed in the middle of the motor carriage (motor coach), near the vestibule, in the electrical apparatus compartment (Figure 4).

The electricity meter, designation EM3000, was manufactured by Sesto Ltd. (sp. z o.o. in Polish) and is a device commonly used in rail transport to measure, among other things, traction voltage and electricity intake (taken) and donated (fed, put, devoted, returned) into the catenary (Figure 4b). The electricity meter (including the shunt) is of accuracy class 1.1., meets the requirements of the standard PN-EN 50463 [80], and records data on traction energy taken and donated at 5 min intervals. The electricity meter (for both EMUs—EN57AKŚ-223 and EN57AKŚ-730) had current calibration certificates.

(**a**) (**b**)

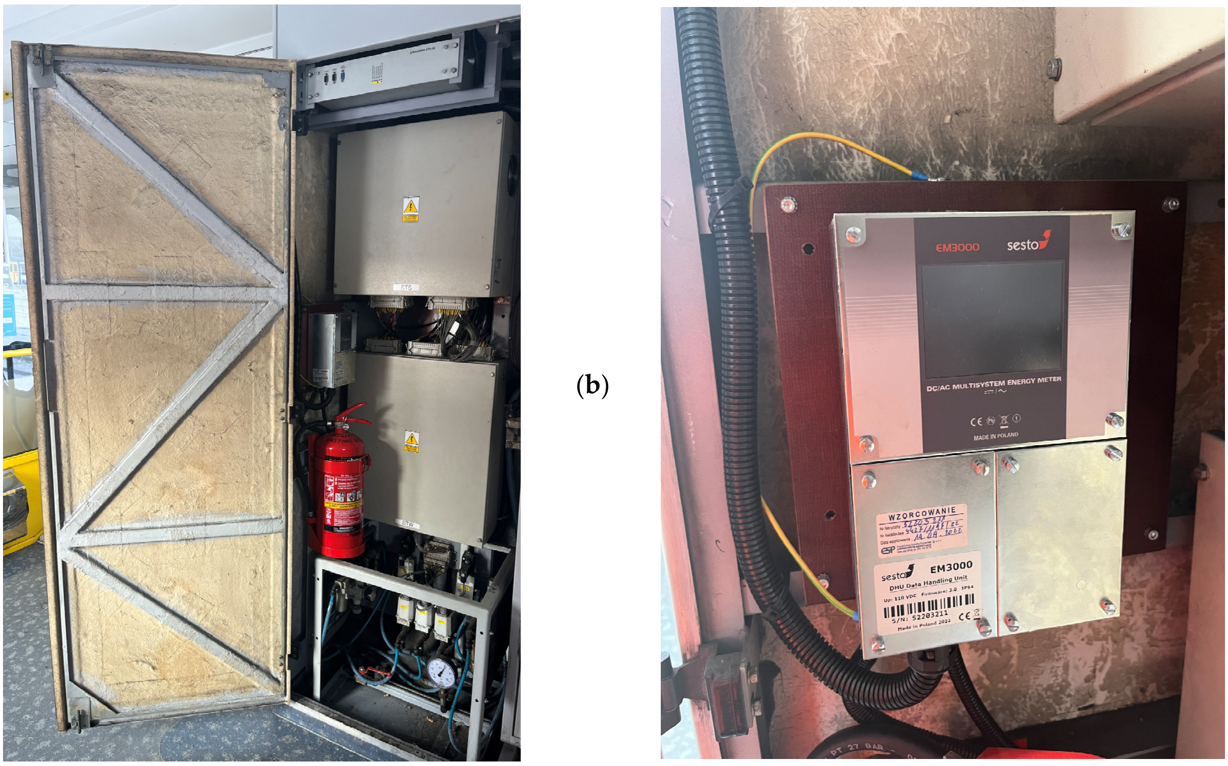

Figure 4. EN57AKŚ-223 series EMU electrical apparatus compartment: (**a**) position of the apparatus; (**b**) electricity meter EM3000.

2.3. Scientific Research and Industry-Specific Methods

In conducting a research study, direct and indirect measurement methods and expert methods are commonly used. DMM and IMM methods are used in the engineering and technical sciences, including civil engineering, surveying/geodesy, and transport, particularly in railway infrastructure and superstructure. The combination of direct and indirect measurement is commonly used in industry-specific and commercial systems. Expert methods, on the other hand, in addition to specific methodologies, require a targeted selection of experts from specific areas and disciplines. EM belongs to the class of heuristic methods. DMM, IMM, and EM are frequently integrated with the following methods:

- Brainstorming: used to create ideas and associations for solving specific problems by scientific research and project teams. The success of BM correlates with the activity of the whole team. BM is a heuristic method;
- Mind mapping: used to identify, define, and record the main subject and develop new and related ideas. It takes into account the use of keywords as well as the hierarchy of concepts. As a result of reflections and creative ideas, a knowledge map is generated using concepts, drawings, short phrases, and other items. MMM is a heuristic method;
- Systems approach, which represents systems thinking. This approach is focused on the big picture and the interaction between the individual elements of the whole;
- Heuristic method, which unifies various ways and rules of conduct for making sound decisions in difficult situations. The heuristic method requires defining a problem, formulating a hypothesis, collecting and analyzing data, and obtaining conclusions;
- Failure mode and effect analysis: designed to prevent the consequences and effects of defects, its purpose is to prevent failures.

The integration of these methods reflects the level of complexity involved in the realization of the project objectives and their presentation. The project of integrating TE consumption determinants with the route geometry and vehicle characteristics was completed using the following:

1. Variant I, the existing approach, which involves calculating the values of electricity consumption q and the total specific energy consumption measured at the motor terminals j_0 for individual component segments and the complete route. The approach is considered prevalent to date, according to [59].
2. Variant II, the new approach, which involves calculating the values of electricity consumption q_i and the total specific energy consumption measured at the motor terminals j_i for individual component segments and the complete route [59–61]. It was used to complete the following:
   - Measuring electricity consumption during braking for JRT ($q_{JRT\ braking}$ and $j_{0JRT\ braking}$), aligned with [62];
   - Measuring electricity consumption during braking on CWR track ($q_{CWRt\ braking}$ and $j_{0CWRt\ braking}$), aligned with [62];
   - Measuring electricity consumption during startup on JRT ($q_{JRT\ startup}$ and $j_{0JRT\ startup}$);
   - Measuring electricity consumption during startup on CWR track ($q_{CWRt\ startup}$ and $j_{0CWRt\ startup}$).

   The project also integrated relevant summer and winter seasonal data.

3. Results

3.1. Traction Electricity Consumption to Date

Burak-Romanowski and Woźniak [59] focused on the subject of traction electricity consumption expressed in Equation (1), so-called Variant I, the existing and so far prevalent calculation method. In Variant I, integration of traction electricity consumption q determinants with route geometry and the vehicle is defined in Equation (1) [59] as follows:

$$q = 2.725\left(w_0 + w_B + i_{sp} \pm \frac{h}{S} + \frac{V_t V_m}{100K}\right) + \frac{1.073}{L}\left[k'\left(\frac{V_h}{10}\right)^2 + \varphi k''\left(\frac{V_r}{10}\right)^2\right] \quad \left[\frac{\mathrm{W{\cdot}h}}{\mathrm{t{\cdot}km}}\right] \tag{1}$$

where w_0 is a fixed resistance factor, w_B is resistance to curvature (for flat terrain and mountainous terrain, respectively), K is the train type factor, V_t is technical speed (average), V_m is the maximum speed of passenger trains, h is the difference in level between the end station and the start station, S is the distance between the start and end railway stations, i_{sp} is the average additional movement resistance caused by braking, φ is the loss factor in resistors during startup, V_h is braking start speed, V_r is the final startup speed, L is route length, k' is a factor such that k' = 1 for all trains, and k'' is a coefficient such that k'' = 1.2 for passenger trains and k'' = 1.4 for freight trains.

In order to calculate the q values for the linear objects represented by the railway line segments in interaction with the EMUs, the actual values for speed were determined based on the data recorded by the catenary-supplied electric vehicles' onboard recorders. These values were determined using the average of four journeys along the complete Lubliniec–Katowice route used in the study of EN57AKŚ-730 and EN57AKŚ-223 vehicles. The complete approach ensured that real values were obtained for technical speed (average) V_t, maximum speed, speed of passenger trains V_m, and braking start speed V_h, applicable to the further calculations of all 16 railway segments included in the study. The value V_r, final startup speed, was 40 km/h, according to the EMUs technical documentation used in the study. The value of the parameter w_0 (fixed resistance factor) was assumed to be 2 and was adopted for passenger trains. Parameter value w_B (resistance to curvature) was adopted at the level of 0.31 (adequate for plain terrain because of relatively small differences in elevation between the railway segments, amounting, for example, to h_{m1} of 57.32 m between the route starting point 1 at Lubliniec and point 7 at Nakło Śląskie, which is the greatest elevation difference). Because of the slight gradient of the different segments of the railway lines and the consequent values of i_x for each case being less than the value of w_x, in further calculations, the i_{sp} value for all segments was assumed to be 0. Values h (the difference in elevation between the end railway station and the start railway station) and S (distance between the start and end railway stations) were selected on the basis of the actual values for each segment of the Lubliniec–Katowice line. K-factor (train type) was adopted at the level of 25 (corresponding to the average length of the unit depots, which include the EN57AKŚ series EMUs with a length of 64.77 m). Value L (route length) was taken to be equal to the value of S, which combines individual railway line segments (stations and passenger stops), outside of which there are no additional stops. The value for parameter φ (loss factor in resistors during startup) was taken to be 0.55 and adopted for four-engine vehicles (such as EN57AKŚ vehicles). The last of the parameters, i.e., the k'' factor, was 1.2, based on the type of transport operations, while the value of the k' factor was 1.

Given the difference in the efficiency of the transmission (gearbox, gear) and engine in the vehicle, Table 2 shows the total specific energy consumption measured at the motor terminals, calculated and identified in Variant I as the value of j_0 expressed by Equation (2) [59]:

$$j_0 = \frac{q}{\eta \cdot \eta_z} \left[\frac{\mathrm{W \cdot h}}{\mathrm{t \cdot km}}\right] \quad (2)$$

where η is the engine efficiency (adopted at 0.90), and η_z is the mechanical transmission efficiency (adopted at 0.97).

Table 2. Variant I: calculated electricity consumption values q, j_0, and E_{Iwe}.

Segment Designation	Name of Linear Objects	q $[\frac{\mathrm{W \cdot h}}{\mathrm{t \cdot km}}]$	j_0 $[\frac{\mathrm{W \cdot h}}{\mathrm{t \cdot km}}]$	E_{Iwe} [kWh]
1–2	Lubliniec–Rusinowice	33.34	38.19	28.00
2–3	Rusinowice–Koszęcin	34.17	39.14	28.59
3–4	Koszęcin–Kalety	30.69	35.15	31.82
4–5	Kalety–Miasteczko Śląskie	25.65	29.38	28.68
5–6	Miasteczko Śląskie–Tarnowskie Góry	28.59	32.75	24.25
6–7	Tarnowskie Góry–Nakło Śląskie	43.33	49.63	20.49
7–8	Nakło Śląskie–Radzionków	49.69	56.92	17.45
8–9	Radzionków–Radzionków Rojca	47.10	53.95	11.31
9–10	Radzionków Rojca–Bytom Północny	44.63	51.12	16.74
10–11	Bytom Północny–Bytom Karb	18.57	21.27	7.73
11–12	Bytom Karb–Bytom	18.45	21.14	6.38
12–13	Bytom–Chorzów Stary	27.39	31.38	16.27
13–14	Chorzów Stary–Chorzów Miasto	27.44	31.43	7.97
14–15	Chorzów Miasto–Chorzów Batory	19.57	22.42	6.42
15–16	Chorzów Batory–Katowice Załęże	37.14	42.54	19.44
16–17	Katowice Załęże–Katowice	35.89	41.11	10.60
	SUM			282.13

In Table 2, the calculated values of electricity consumption are summarized by q, and the total specific energy consumption was measured at the motor terminals j_0 for Variant I using Equations (1) and (2) [59] for individual segments and the complete route. Table 2 contains the determined values of electric energy consumption E_{Iwe} for the actual value of the vehicle weight (124 tons) and the actual distances of segments, determined on the basis of j_0.

3.2. Traction Electricity Consumption: A New Approach during Braking

3.2.1. Braking on Jointed Railway Track

The purpose was to calculate the traction energy consumption during braking of catenary-supplied electric vehicles on jointed railway tracks ($q_{JRT\ braking}$) and the total specific energy consumption measured at the motor terminals ($j_{0JRT\ braking}$) in a new approach called Variant II, referencing Equations (1) and (2) [59], and in correspondence with [62]. Taking into account the relative value of the movement resistance force during braking on jointed railway tracks $M_{res\ JRT\ braking}$, in correspondence with [60,61], we obtained Equation (3):

$$q_{JRT\ braking} = 2.725\left(w_0 + w_B + M_{res\ JRT\ braking} \pm \frac{h}{S} + \frac{V_t V_m}{100K}\right) + \frac{1.073}{L}\left[k'\left(\frac{V_h}{10}\right)^2 + \varphi k''\left(\frac{V_r}{10}\right)^2\right]\left[\frac{\mathrm{W\cdot h}}{\mathrm{t\cdot km}}\right] \quad (3)$$

where $M_{res\ JRT\ braking}$ is a relative value of the movement resistance force during braking on jointed railway track with respect to vehicle speed V in $\left[\frac{m}{s}\right]$ (average speed of the vehicles recorded by their driving data recorder) expressed by Equation (4) [60,61]:

$$M_{res\ JRT\ braking} = 2.4 + 0.011V + 0.00035V^2\left[\frac{N}{t}\right] \quad (4)$$

The total specific energy consumption measured at the motor terminals $j_{0JRT\ braking}$ was calculated using Equation (2), taking a new approach during braking on jointed railway tracks into account for the values of $q_{JRT\ braking}$ expressed by Equation (3).

In Table 3, the calculated values of electricity consumption are summarized by $q_{JRT\ braking}$ and the total specific energy consumption measured at the motor terminals is represented by $j_{0JRT\ braking}$ for Variant II for JRT individual segments and the complete route. Table 3 contains the determined values of electric energy consumption $E_{IIweJRT\ braking}$ calculated for the actual vehicle weight (124 tons) and the actual distance segments based on the $j_{0JRT\ braking}$.

Table 3. Calculated electricity consumption values $q_{JRT\ braking}$, $j_{0JRT\ braking}$ and $E_{IIweJRT\ braking}$ (Variant II, the new approach for braking on jointed railway tracks).

Segment Designation	Name of Linear Objects	$q_{JRT\ braking}$ $\left[\frac{\mathrm{W\cdot h}}{\mathrm{t\cdot km}}\right]$	$j_{0JRT\ braking}$ $\left[\frac{\mathrm{W\cdot h}}{\mathrm{t\cdot km}}\right]$	$E_{IIweJRT\ braking}$ [kWh]
1–2	Lubliniec–Rusinowice	48.77	55.86	40.95
2–3	Rusinowice–Koszęcin	50.72	58.10	42.43
3–4	Koszęcin–Kalety	44.37	50.82	46.00
4–5	Kalety–Miasteczko Śląskie	44.23	50.66	49.46
5–6	Miasteczko Śląskie–Tarnowskie Góry	42.74	48.96	36.25
6–7	Tarnowskie Góry–Nakło Śląskie	72.93	83.54	34.50
7–8	Nakło Śląskie–Radzionków	69.69	79.82	24.47
8–9	Radzionków–Radzionków Rojca	50.65	58.02	12.17
9–10	Radzionków Rojca–Bytom Północny	37.33	42.76	14.00
10–11	Bytom Północny–Bytom Karb	27.33	31.31	11.37
11–12	Bytom Karb–Bytom	17.72	20.30	6.13
12–13	Bytom–Chorzów Stary	54.58	62.52	32.41
13–14	Chorzów Stary–Chorzów Miasto	44.02	50.42	12.78
14–15	Chorzów Miasto–Chorzów Batory	13.51	15.47	4.43
15–16	Chorzów Batory–Katowice Załęże	53.93	61.77	28.22
16–17	Katowice Załęże–Katowice	46.70	53.49	13.79
	SUM			409.36

3.2.2. Braking on Continuous Welded Rail Track

Calculation of the traction energy consumption during braking of catenary-supplied electric vehicles on continuous welded rail tracks $q_{CWRbraking}$ and the total specific energy consumption measured at the motor terminals $j_{0CWRbraking}$ was carried out using Variant II with reference to the equations (1) and (2) [59], in correspondence with [62]. Applying the relative value of the movement resistance force during braking on continuous welded rail tracks $M_{res\ CWRt\ braking}$ in correspondence with [60,61], we obtained Equation (5):

$$q_{CWRt\ braking} = 2.725\left(w_0 + w_B + M_{res\ CWRt\ braking} \pm \frac{h}{S} + \frac{V_t V_m}{100K}\right) + \frac{1.073}{L}\left[k'\left(\frac{V_h}{10}\right)^2 + \varphi k''\left(\frac{V_r}{10}\right)^2\right]\left[\frac{\mathrm{W\cdot h}}{\mathrm{t\cdot km}}\right] \quad (5)$$

where $M_{res\ CWRt\ braking}$ is a relative value of the movement resistance force during braking on continuous welded rail tracks with respect to vehicle speed V in $\left[\frac{m}{s}\right]$ (average speed of the vehicles recorded by their driving data recorder), expressed by Equation (6) [60,61]:

$$M_{res\ CWRt\ braking} = 2.4 + 0.009V + 0.00035V^2 \left[\frac{N}{t}\right] \tag{6}$$

The total specific energy consumption measured at the motor terminals $j_{0CWRt\ braking}$ was calculated using Equation (2), taking into account the new approach during braking on continuous welded rail tracks for the values of $q_{CWRt\ braking}$ expressed by Equation (5).

In Table 4, the calculated electricity consumption values are summarized by $q_{CWRt\ braking}$ and the total specific energy consumption measured at the motor terminals is presented as $j_{0CWRt\ braking}$ for Variant II for CWRt individual segments and the complete route. Table 4 contains the determined values of electric energy consumption $E_{IIweCWRt\ braking}$ for the actual vehicle weight (124 tons) and the actual distance segments based on $j_{0CWRt\ braking}$.

Table 4. Calculated electricity consumption values $q_{CWRt\ braking}$, $j_{0CWRt\ braking}$ and $E_{IIweCWRt\ braking}$ (Variant II, the new approach during braking on continuous welded rail tracks).

Segment Designation	Name of Linear Objects	$q_{CWRt\ braking}$ $\left[\frac{W\cdot h}{t\cdot km}\right]$	$j_{0CWRt\ braking}$ $\left[\frac{W\cdot h}{t\cdot km}\right]$	$E_{IIweCWRt\ braking}$ [kWh]
1–2	Lubliniec–Rusinowice	48.66	55.74	40.86
2–3	Rusinowice–Koszęcin	50.61	57.97	42.33
3–4	Koszęcin–Kalety	44.25	50.68	45.88
4–5	Kalety–Miasteczko Śląskie	44.11	50.53	49.32
5–6	Miasteczko Śląskie–Tarnowskie Góry	42.64	48.84	36.16
6–7	Tarnowskie Góry–Nakło Śląskie	72.83	83.43	34.45
7–8	Nakło Śląskie–Radzionków	69.59	79.71	24.44
8–9	Radzionków–Radzionków Rojca	50.57	57.93	12.15
9–10	Radzionków Rojca–Bytom Północny	37.24	42.66	13.97
10–11	Bytom Północny–Bytom Karb	27.27	31.23	11.35
11–12	Bytom Karb–Bytom	17.67	20.24	6.11
12–13	Bytom–Chorzów Stary	54.50	62.43	32.36
13–14	Chorzów Stary–Chorzów Miasto	43.95	50.35	12.76
14–15	Chorzów Miasto–Chorzów Batory	13.44	15.40	4.41
15–16	Chorzów Batory–Katowice Załęże	53.83	61.66	28.17
16–17	Katowice Załęże–Katowice	46.63	53.42	13.77
	SUM			408.50

3.3. Traction Electricity Consumption: A New Approach during Startup

3.3.1. Startup on Jointed Railway Track

Calculation of the traction energy consumption during startup of catenary-supplied electric vehicles on jointed railway tracks $q_{JRT\ startup}$ and the total specific energy consumption measured at the motor terminals $j_{0JRT\ startup}$ was carried out using Variant II with reference to Equations (1) and (2) [59]. Taking into account the relative value of the movement resistance force during startup on jointed railway tracks $M_{res\ JRT\ startup}$ in correspondence with [60,61], we obtained Equation (7):

$$q_{JRT\ startup} = 2.725\left(w_0 + w_B + M_{res\ JRT\ startup} \pm \frac{h}{S} + \frac{V_t V_m}{100K}\right) + \frac{1.073}{L}\left[k'\left(\frac{V_h}{10}\right)^2 + \varphi k''\left(\frac{V_r}{10}\right)^2\right]\left[\frac{W\cdot h}{t\cdot km}\right] \tag{7}$$

where $M_{res\ JRT\ startup}$ is the relative value of the movement resistance force during startup on jointed railway tracks with respect to vehicle speed V in $\left[\frac{m}{s}\right]$ (average speed of the vehicles recorded by their driving data recorder), expressed by Equation (8) [60,61]:

$$M_{res\ JRT\ startup} = 1.9 + 0.01V + 0.0003V^2 \left[\frac{N}{t}\right] \tag{8}$$

The total specific energy consumption measured at the motor terminals $j_{0JRT\ startup}$ was calculated using Equation (2), taking into account the values of $q_{JRT\ startup}$ expressed by Equation (7).

In Table 5, the calculated electricity consumption values are summarized under $q_{JRT\ startup,}$ along with the total specific energy consumption measured at the motor terminals under $j_{0JRT\ startup}$ for Variant II during startup for JRT individual segments and the complete route. Table 5 contains the determined values of electric energy consumption $E_{IIweJRT\ startup}$ for the actual vehicle weight (124 tons) and the actual distance segments based on the $j_{0JRT\ startup}$.

Table 5. Calculated electricity consumption values $q_{JRT\ startup}$, $j_{0JRT\ startup}$ and $E_{IIweJRT\ startup}$ (Variant II, the new approach during startup on jointed railway tracks).

Segment Designation	Name of Linear Objects	$q_{JRT\ startup}$ $\left[\frac{W\cdot h}{t\cdot km}\right]$	$j_{0JRT\ startup}$ $\left[\frac{W\cdot h}{t\cdot km}\right]$	$E_{IIweJRT\ startup}$ [kWh]
1–2	Lubliniec–Rusinowice	47.30	54.18	39.72
2–3	Rusinowice–Koszęcin	49.24	56.40	41.19
3–4	Koszęcin–Kalety	42.88	49.12	44.46
4–5	Kalety–Miasteczko Śląskie	42.74	48.96	47.80
5–6	Miasteczko Śląskie–Tarnowskie Góry	41.28	47.29	35.01
6–7	Tarnowskie Góry–Nakło Śląskie	71.48	81.88	33.81
7–8	Nakło Śląskie–Radzionków	68.23	78.16	23.96
8–9	Radzionków–Radzionków Rojca	49.22	56.38	11.82
9–10	Radzionków Rojca–Bytom Północny	35.88	41.10	13.46
10–11	Bytom Północny–Bytom Karb	25.92	29.69	10.79
11–12	Bytom Karb–Bytom	16.32	18.69	5.65
12–13	Bytom–Chorzów Stary	53.15	60.88	31.56
13–14	Chorzów Stary–Chorzów Miasto	42.60	48.80	12.37
14–15	Chorzów Miasto–Chorzów Batory	12.10	13.86	3.97
15–16	Chorzów Batory–Katowice Załęże	52.48	60.11	27.46
16–17	Katowice Załęże–Katowice	45.28	51.87	13.37
	SUM			396.39

3.3.2. Startup on Continuous Welded Rail Tracks

Calculation of the traction energy consumption during startup of catenary-supplied electric vehicles on continuous welded rail tracks $q_{CWRt\ startup}$ and the total specific energy consumption measured at the motor terminals $j_{0CWRt\ startup}$ was carried out using the Variant II approach, with reference to Equations (1) and (2) [59]. Taking into account the relative value of the movement resistance force during startup on continuous welded rail tracks $M_{res\ CWRt\ startup}$, in correspondence with [60,61], we obtained Equation (9):

$$q_{CWRt\ startup} = 2.725\left(w_0 + w_B + M_{res\ CWRt\ startup} \pm \frac{h}{S} + \frac{V_t V_m}{100K}\right) + \frac{1.073}{L}\left[k'\left(\frac{V_h}{10}\right)^2 + \varphi k''\left(\frac{V_r}{10}\right)^2\right]\left[\frac{\mathrm{W\cdot h}}{\mathrm{t\cdot km}}\right] \tag{9}$$

where $M_{res\ CWRt\ startup}$ is the relative value of the movement resistance force during startup on continuous welded rail tracks with respect to vehicle speed V in $\left[\frac{m}{s}\right]$ (average speed of the vehicles recorded by their driving data recorder), expressed by Equation (10) [60,61]:

$$M_{res\ CWRt\ startup} = 1.9 + 0.008V + 0.00025V^2 \left[\frac{N}{t}\right] \quad (10)$$

The total specific energy consumption measured at the motor terminals $j_{0CWRt\ startup}$ was calculated using Equation (2), taking a new approach during startup on continuous welded rail tracks into account for the values of $q_{CWRt\ startup}$ expressed by Equation (9).

In Table 6, the calculated electricity consumption values are summarized under $q_{CWRt\ startup}$, and the total specific energy consumption measured at the motor terminals is summarized under $j_{0CWRt\ startup}$ for Variant II for CWRt individual segments and the complete route. Table 6 contains the determined values of electric energy consumption $E_{IIweCWRt\ startup}$ for the actual vehicle weight (124 tons) and the actual distance segments based on $j_{0CWRt\ startup}$.

Table 6. Calculated electricity consumption values $q_{CWRt\ startup}$, $j_{0CWRt\ startup}$, and $E_{IIweCWRt\ startup}$ (Variant II, the new approach during startup on continuous welded rail tracks).

Segment Designation	Name of Linear Objects	$q_{CWRt\ startup}$ $\left[\frac{W \cdot h}{t \cdot km}\right]$	$j_{0CWRt\ startup}$ $\left[\frac{W \cdot h}{t \cdot km}\right]$	$E_{IIweCWRt\ startup}$ [kWh]
1–2	Lubliniec–Rusinowice	22.48	25.75	39.58
2–3	Rusinowice–Koszęcin	47.14	53.99	41.04
3–4	Koszęcin–Kalety	49.06	56.20	44.27
4–5	Kalety–Miasteczko Śląskie	42.70	48.91	47.59
5–6	Miasteczko Śląskie–Tarnowskie Góry	42.56	48.75	34.88
6–7	Tarnowskie Góry–Nakło Śląskie	41.13	47.11	33.75
7–8	Nakło Śląskie–Radzionków	71.35	81.72	23.92
8–9	Radzionków–Radzionków Rojca	68.10	78.01	11.80
9–10	Radzionków Rojca–Bytom Północny	49.11	56.26	13.42
10–11	Bytom Północny–Bytom Karb	35.76	40.96	10.75
11–12	Bytom Karb–Bytom	25.84	29.60	5.62
12–13	Bytom–Chorzów Stary	16.25	18.61	31.49
13–14	Chorzów Stary–Chorzów Miasto	53.03	60.75	12.34
14–15	Chorzów Miasto–Chorzów Batory	42.52	48.71	3.94
15–16	Chorzów Batory–Katowice Załęże	12.02	13.76	27.39
16–17	Katowice Załęże–Katowice	52.34	59.95	13.35
	SUM			395.13

3.4. Real Traction Electricity Consumption in Correlation with the Seasons: Traction Electric Vehicle Recorders

Real traction electricity consumption of EN57AKŚ-730 and EN57AKŚ-223 vehicles was monitored using electricity meters installed in these EMUs. Measurements were taken in winter and summer during journeys along the Lubliniec–Katowice route. Because of the vehicle construction characteristics, we also monitored the possibility of recuperating electricity, which could be returned/generated through the electrodynamic braking process to the catenary. However, the amount of energy put into the catenary directly depends on the ability of another vehicle in the vicinity to receive it; therefore, these data are partially random. Nevertheless, the data may prove relevant in future studies and were thus deemed important to note. Monitoring was carried out for 19 journeys along the complete route each month, and EMUs were represented by EN57AKŚ-223 and EN57AKŚ-730 vehicles. Results are average values for the months under study.

3.4.1. Summer Data

In total, 19 journeys were selected for the summer measurements in July 2021 and 19 journeys in August 2021 for each EMU. All data refer to energy consumption on the total Lubliniec—Katowice route for vehicles EN57AKŚ-223 and EN57AKŚ-730. The values recorded were the energy intake from the catenary E_{we} and the energy devoted to the catenary due to electrodynamic braking E_{wy}. The difference between the two energy values in summer (intake E_{we} and devoted E_{wy}) was also calculated. Average values for individual EMUs are provided in Table 7.

Table 7. Summary of energy intake and return during the summer period.

Electric Multiple Units	Energy Intake E_{we} [kWh]	Energy Returned E_{wy} [kWh]	Difference in Summer E_{we}–E_{wy} [kWh]
	Summer–July 2021		
EN57AKŚ-223	272.26	92.68	179.58
EN57AKŚ-730	348.53	117.84	230.68
	Summer–August 2021		
EN57AKŚ-223	264.11	85.89	178.21
EN57AKŚ-730	344.68	111.63	233.05
	Summer average		
EN57AKŚ-223	268.18	89.29	178.89
EN57AKŚ-730	346.61	114.74	231.87

3.4.2. Winter Data

The same number of journeys were selected to carry out the measurements during the winter period—19 in January 2022 and 19 in February 2022 for each of the EMUs. All monitored data include the energy consumption of the complete Lubliniec–Katowice journey of the EN57AKŚ-223 and EN57AKŚ-730 vehicles.

The values recorded were the energy intake from the catenary E_{we} and the energy devoted to the catenary due to electrodynamic braking E_{wy}. The difference between the two energy values in winter (intake E_{we} and devoted E_{wy}) was also calculated. Average values for individual EMUs are provided in Table 8.

Table 8. Summary of energy intake and return during the winter period.

Electric Multiple Units	Energy Intake E_{we} [kWh]	Energy Returned E_{wy} [kWh]	Difference in Winter E_{we}–E_{wy} [kWh]
	Winter–January 2022		
EN57AKŚ-223	387.16	92.16	295.00
EN57AKŚ-730	398.42	88.05	310.37
	Winter–February 2022		
EN57AKŚ-223	373.26	94.21	279.05
EN57AKŚ-730	372.37	91.42	280.95
	Winter average		
EN57AKŚ-223	380.21	93.18	287.03
EN57AKŚ-730	385.39	89.74	295.66

3.5. Comparative Analysis and Evaluation of the Values Obtained

The results of electricity consumption, determined with Variant I and Variant II (both for braking work and startup), in the case of JRT and CWRt, were compared with each other and with the electricity consumed by EN57AKŚ-223 and EN57AKŚ-730. An average value for the actual electricity consumption was determined for both vehicles. A comparison of electricity consumption for the described variants is presented in Figure 5.

The comparative analysis and evaluation show that the new method (Variant II) allows us to obtain results very close to the real values recorded by the electricity meters installed on the vehicles. However, it is also worth noting that in the case of actual energy consumption in the summer period, the calculation method used in Variant I obtained the values closest to the real ones.

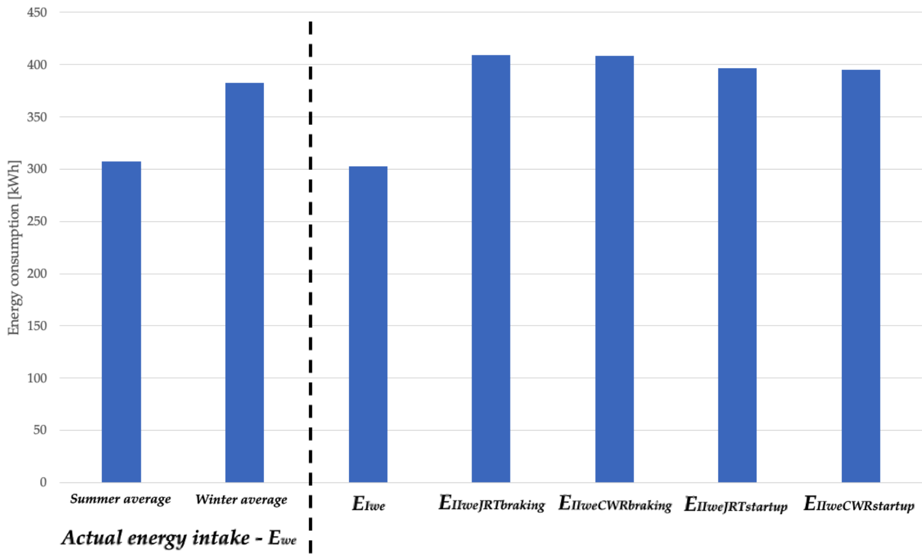

Figure 5. Comparison of electricity consumption for EN57AKŚ: Lubliniec–Katowice route where vertical dashed line — exposure: real traction electricity consumption in correlation with the seasons (left side) in relation to Variant I and II (right side).

Because the data in Figure 5 represent electricity consumption, assuming that the complete route has a JRT or CWRt construction, it was necessary to relate the calculated values of electricity consumption to the actual types of railway construction in the analyzed segments. Thus, Table 9 shows the energy consumption values in relation to the actual railway track construction on individual segments of the railway line. Energy consumption values were determined as the average values obtained from braking and startup calculations.

Table 9. Energy consumption depending on the type of railway track.

Segment Designation	Name of Linear Objects	Railway Track Type	$E_{IIwe\ braking}$ [kWh]	$E_{IIwe\ startup}$ [kWh]	$E_{IIwe\ Average}$ [kWh]
1–2	Lubliniec–Rusinowice	CWRt	40.86	39.58	40.22
2–3	Rusinowice–Koszęcin	CWRt	42.33	41.04	41.69
3–4	Koszęcin–Kalety	CWRt	45.88	44.27	45.08
4–5	Kalety–Miasteczko Śląskie	CWRt	49.32	47.59	48.46
5–6	Miasteczko Śląskie–Tarnowskie Góry	CWRt	36.16	34.88	35.52
6–7	Tarnowskie Góry–Nakło Śląskie	CWRt	34.45	33.75	34.10
7–8	Nakło Śląskie–Radzionków	CWRt	24.44	23.92	24.18
8–9	Radzionków–Radzionków Rojca	CWRt	12.15	11.80	11.98
9–10	Radzionków Rojca–Bytom Północny	CWRt	13.97	13.42	13.70
10–11	Bytom Północny–Bytom Karb	JRT	11.37	10.79	11.08
11–12	Bytom Karb–Bytom	JRT	6.13	5.65	5.89
12–13	Bytom–Chorzów Stary	CWRt	32.36	31.49	31.93
13–14	Chorzów Stary–Chorzów Miasto	JRT	12.78	12.37	12.58
14–15	Chorzów Miasto–Chorzów Batory	JRT	4.43	3.97	4.20
15–16	Chorzów Batory–Katowice Załęże	CWRt	28.17	27.39	27.78
16–17	Katowice Załęże–Katowice	CWRt	13.77	13.35	13.56
		SUM			401.92

The average value of the calculated energy consumption $E_{IIwe\ Average}$, taking into account the actual construction of the individual segments of the railway track presented in Table 9, is also shown in Figure 6 graph with the average value of energy consumed from the catenary (based on data from the electricity meter) for the winter and summer period. These values are very close. The new approach of Variant II provides a wide scope for monitoring the status of total traction electricity consumption of the route depending on the railway track construction, particularly on routes equipped with different constructions, such as JRT and CWRt. Another important aspect is its application during repairs, e.g., railway track installation, especially during the process of revitalization, modernization, construction of new linear objects and investment processes, as well as during temporary maintenance of the JRT and until the completion of the CWRt implementation process, etc.

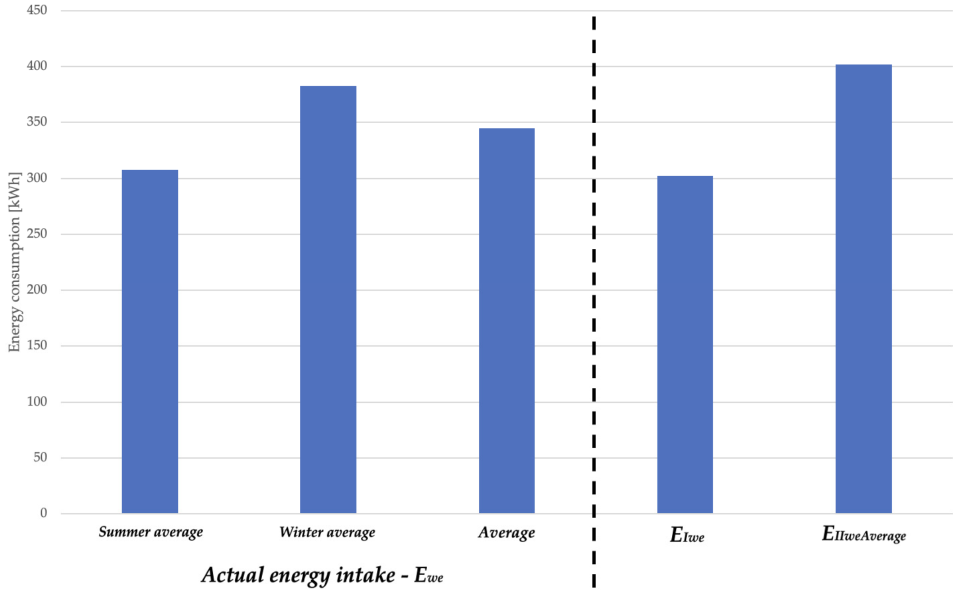

Figure 6. Comparison of electricity consumption based on the actual railway track construction, where vertical dashed line—exposure: real traction electricity consumption in correlation with the seasons (left side) in relation to Variant I and II (right side).

Figure 7 shows the graph of railway catenary-supplied electric vehicles' speeds in km/h and energy consumption $E_{IIwe\ Average}$ as a function of the distance between individual component segments and the complete route. Speeds were determined as average values based on data from onboard speed recorders from all researched vehicles. There is a clear correlation between the increase in the average speed and the increase in the amount of energy consumed in both CWRt and JRT, also reflective of the railway track construction type.

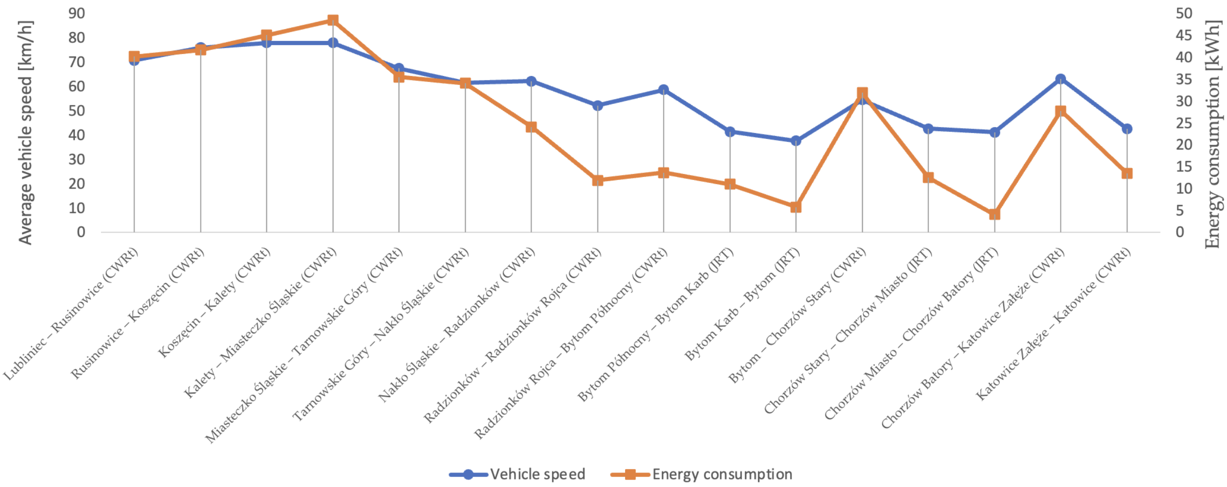

Figure 7. Correlation of traction electricity consumption in relation to average catenary-supplied electric vehicles speeds and travel distance along the complete route and the individual component of CWRt and JRT.

4. Discussion

This study integrates determinants of traction electricity consumption with the route geometry and vehicle characteristics. It reveals ideas, interpretations, and, more importantly, recommendations for other international scientific research studies and industry works with a common denominator. The results of our study represent the logical synthesis of research and observational data and industry-specific methods in an innovative and applicable approach.

Fischer and Szürke [14], investigating the causes of energy loss and reasons for high energy consumption, found that the driving style and habits of the train operators were among their primary causes. Scheepmaker et al. [81] also recognized this, emphasizing that the drivers' train driving strategy significantly impacts energy consumption. Undoubtedly, this is also correlated with work carried out in the industry. However, the work undertaken in this study offers a step forward that can significantly advance the knowledge and methods applied in scientific research and industry works, especially in train driving strategies.

Authors rightly emphasize Kuźmiński et al. [82], stating that transport solutions should be optimized. At the same time, they point out that the rapid growth of the world's population and the associated increase in the number of vehicles are reflected in the increase in traffic, which will continue to grow, making the subject of traffic jams increasingly critical [82]. The solution here is rail transport, which requires proper monitoring but has many advantages. Wojtaszek and Miciuła [83] stated that exploring the various determinants important for enhancing innovation is legitimate. Therefore, the chosen subject and the scope of work carried out in this study can be considered valid. Żywiołek et al. [84] claimed that energy saving is now a popular research topic, although the specific effects of energy conservation awareness are still being studied. It should be emphasized that the authors of [84] found that energy savings are influenced not only by economic factors but also by an informed public which cares about managing resources. Their results agree with Ibrahim and Jiang [85], who, referring to electric vehicle energy management, stressed the need for good energy management consisting of optimization of the design and operation of the vehicle energy system. Our work on integrating TE consumption determinants with the route geometry and vehicle characteristics, especially with regard to the new approaches implemented for JRT and CWRt, echoes their theme of route and vehicle geometry maintenance with a common denominator in energy management. Thus, there is a constructive correlation between route geometry and the railway catenary vehicle, especially with respect to power system operation, control, stability, and advances in electrical engineering. Heirich et al. [57] dealt with RailSLAM, responsible for the creation and maintenance of the special track map using simultaneous estimation of probabilistic geometric and topological track features and train states, referred to as the global navigation satellite system (GNSS) and a low-cost MEMS inertial measurement unit (IMU). The GNSS technology is also referred to by Maciuk [86,87], who noted that it plays an important role in civil engineering. Jánešová and Kratochvil [88] related it to creating an economic–mathematical model for the web portal. It is undoubtedly worth considering the integration of the results of scientific research work. Thus, the development of GNSS, in combination with other technologies, parallels the integration of traction electricity consumption determinants with the route geometry and vehicle characteristics and advances it in support of sustainability development.

According to the scientific research presented here, atmospheric factors influence the amount of electricity consumption. This additional information can be used to build predictive models, as emphasized by Zalewski [8]. It is also important to acknowledge the statement of González-Gil et al. [89] highlighting the role of urban rail transport as a key contributor to sustainable development, especially in the 'society characterized by increasing rates of urbanization and growing concerns about environmental issues like climate change'. The present study and the implementation of its results will help fill the current gap between research and practice by bringing together the theoretical work on integrating traction electricity consumption determinants, route geometry, and vehicle characteristics with the practical work on actual traction electricity consumption in correlation with the relevant seasonal data.

The new approach presented here has the potential to monitor the traction electricity consumption of traction electric vehicles and whole trains in rail transport.

5. Conclusions

Finally, we can state that the aim of our research project was achieved. The results of the work carried out and the implementation of the new approaches show that their proper implementation already contributes to and will continue to improve the efficiency of integrating TE consumption determinants and route geometry and vehicle characteristics. The new approach certainly has potential, especially for monitoring TE consumption of rail transport infrastructure equipped with JRT or CWRt.

In this paper, we present an innovative approach to monitoring the state of traction electricity consumption for rail transport determined by factors related to the characteristics of the route geometry (railway lines) and the characteristics of traction electric vehicles and trains. These determinants correlate with each other and impact driving speed, which, in turn, affects energy consumption. Two approaches/variants were completed in this study:

1. Variant I—the approach most frequently used to date;
2. Variant II—the new approach.

Variant II, concentrating on the integration of traction electricity consumption determinants and route geometry and vehicle characteristics, ensures the monitoring of electric energy consumption q_i, including total specific energy consumption measured at the motor terminals j_i. The new approach uses values for the movement resistance of electric locomotives during braking on jointed railway tracks $M_{res\ JRT\ braking}$ and continuous welded rail tracks $M_{res\ CWRt\ braking}$ and applies the values of the movement resistance of the electric locomotives during startup on jointed railway tracks to $M_{res\ JRT\ startup}$ and continuous welded rail tracks $M_{res\ CWRt\ startup}$.

The obtained results also integrate the seasonal data for summer and winter, as the actual energy consumption recorded by the EMUs' onboard electricity meters, allowing us to obtain satisfactory results. Variant II—the new approach—provides solutions that enhance resource management, particularly by correlating the traction electricity consumption determinants and route geometry and vehicle characteristics, becoming a valuable and innovative tool. Increased awareness of the impact of the traction electricity consumption determinants in correlation with route geometry and vehicle characteristics leads to resource management solutions.

The work completed and implemented in this study, as part of modern power network management, presents advanced solutions, especially for situational awareness and real-time monitoring of its condition. It also provides great opportunities to specifically monitor the total traction electricity consumption dependent on the railway track design. It provides applications for design, realization, exploitation and other investment processes.

Author Contributions: Conceptualization, A.K. (40%), W.G. (30%), and K.G. (30%); methodology, A.K. (40%), W.G. (30%), and K.G. (30%); software, A.K. (10%), W.G. (45%), and K.G. (45%); validation, A.K. (10%), W.G. (45%), and K.G. (45%); formal analysis, A.K. (34%), W.G. (33%), and K.G. (33%); investigation, A.K. (32%), W.G. (34%), and K.G. (34%); resources, A.K. (26%), W.G. (37%), and K.G. (37%); data curation, A.K. (10%), W.G. (45%), and K.G. (45%); writing—original draft preparation, A.K. (34%), W.G. (33%), and K.G. (33%); writing—review and editing, A.K. (50%), W.G. (25%), and K.G. (25%); visualization, A.K. (50%), W.G. (25%), and K.G. (25%); supervision, A.K. (50%); W.G. (25%), and K.G. (25%); project administration, A.K. (60%), W.G. (20%), and K.G. (20%); funding acquisition, A.K. (34%), W.G. (33%), and K.G. (33%). All authors have read and agreed to the published version of the manuscript.

Funding: This research received no external funding.

Institutional Review Board Statement: Not applicable.

Informed Consent Statement: Not applicable.

Data Availability Statement: Not applicable.

Acknowledgments: The article was prepared under the research subvention of the AGH University of Science and Technology, No. 16.16.150.545 in 2023.

Conflicts of Interest: The authors declare no conflict of interest.

References

1. Morlock, F.; Rolle, B.; Bauer, M.; Sawodny, O. Forecasts of Electric Vehicle Energy Consumption Based on Characteristic Speed Profiles and Real-Time Traffic Data. *IEEE Trans. Veh. Technol.* **2019**, *69*, 1404–1418. [CrossRef]
2. Yan, X.; Zhang, R.; Ma, J.; Ma, Y. Considering Variable Road Geometry in Adaptive Vehicle Speed Control. *Math. Probl. Eng.* **2013**, *2013*, 617879. [CrossRef]
3. Ferreira, H.; Rodrigues, C.M.; Pinho, C. Impact of Road Geometry on Vehicle Energy Consumption and CO_2 Emissions: An Energy-Efficiency Rating Methodology. *Energies* **2020**, *13*, 119. [CrossRef]
4. Karwowski, K.; Kuciński, M.; Mizan, M.; Wilk, A. Sieć Sensorowa do Rejestracji Drgań Górnej Sieci Trakcyjnej w Celach Diagnostyki Eksploatacyjnej. *Zesz. Nauk. Wydziału Elektrotechniki I Autom. Politech. Gdańskiej* **2017**, *57*, 43–46.
5. Haładyn, S. The Problem of Train Scheduling in the Context of the Load on the Power Supply Infrastructure. A Case Study. *Energies* **2021**, *14*, 4781. [CrossRef]
6. Song, Y.; Jiang, T.; Nåvik, P.; Rønnquist, A. Geometry Deviation Effects of Railway Catenaries on Pantograph–Catenary Interaction: A Case Study in Norwegian Railway System. *Railw. Eng. Sci.* **2021**, *29*, 350–361. [CrossRef]
7. Boschetti, G.; Mariscotti, A. Integrated Electromechanical Simulation of Traction Systems: Relevant Factors for the Analysis and Estimation of Energy Efficiency. In Proceedings of the 2012 Electrical Systems for Aircraft, Railway and Ship Propulsion, Bologna, Italy, 16–18 October 2012; pp. 1–6. [CrossRef]
8. Zalewski, W. Influence of Weather on the Variability of the Electricity Consumption. *Econ. Manag.* **2011**, *3*, 195–202.
9. Douglas, H.; Roberts, C.; Hillmansen, S.; Schmid, F. An Assessment of Available Measures to Reduce Traction Energy Use in Railway Networks. *Energy Convers. Manag.* **2015**, *106*, 1149–1165. [CrossRef]
10. Su, S.; Tang, T.; Wang, Y. Evaluation of Strategies to Reducing Traction Energy Consumption of Metro Systems Using an Optimal Train Control Simulation Model. *Energies* **2016**, *9*, 105. [CrossRef]
11. Lin, X.; Zhang, G.; Wei, S. Velocity Prediction Using Markov Chain Combined with Driving Pattern Recognition and Applied to Dual-Motor Electric Vehicle Energy Consumption Evaluation. *Appl. Soft Comput.* **2021**, *101*, 106998. [CrossRef]
12. Ćwil, M.; Bartnik, W.; Jarzębowski, S. Railway Vehicle Energy Efficiency as a Key Factor in Creating Sustainable Transportation Systems. *Energies* **2021**, *14*, 5211. [CrossRef]
13. Ahmed, C.; Nur, K.; Ochieng, W. GIS and Genetic Algorithm Based Integrated Optimization for Rail Transit System Planning. *J. Rail Transp. Plan. Manag.* **2020**, *16*, 100222. [CrossRef]
14. Fischer, S.; Szürke, S.K. Detection Process of Energy Loss in Electric Railway Vehicles. *Facta Univ. Ser. Mech. Eng.* **2022**, 1–19. [CrossRef]
15. Fischer, S. Traction Energy Consumption of Electric Locomotives and Electric Multiple Units at Speed Restrictions. *Acta Tech. Jaurinensis* **2015**, *8*, 240–256. [CrossRef]
16. Naldini, F.; Pellegrini, P.; Rodriguez, J. Real-Time Optimization of Energy Consumption in Railway Networks. *Transp. Res. Procedia* **2022**, *62*, 35–42. [CrossRef]
17. Ren, J.; Zhang, Q.; Liu, F. Analysis of Factors Affecting Traction Energy Consumption of Electric Multiple Unit Trains Based on Data Mining. *J. Clean. Prod.* **2020**, *262*, 121374. [CrossRef]
18. Jefimowski, W. Comparative Analysis of Consuming Energy by High Speeds Trains Depending on the Applied Power Supply System. *TTS Tech. Transp. Szyn.* **2014**, *21*, 48–51.
19. Spiryagin, M.; Wu, Q.; Polach, O.; Thorburn, J.; Chua, W.; Spiryagin, V.; Stichel, S.; Shrestha, S.; Bernal, E.; Ahmad, S.; et al. Problems, Assumptions and Solutions in Locomotive Design, Traction and Operational Studies. *Railw. Eng. Sci.* **2022**, *30*, 265–288. [CrossRef]
20. Croce, A.I.; Musolino, G.; Rindone, C.; Vitetta, A. Traffic and Energy Consumption Modelling of Electric Vehicles: Parameter Updating from Floating and Probe Vehicle Data. *Energies* **2022**, *15*, 82. [CrossRef]
21. Sysyn, M.; Gerbera, U.; Gruen, D.; Nabochenko, O.; Kovalchuk, V. Modelling and Vehicle Based Measurements of Ballast Settlements Under the Common Crossing. *Eur. Transp.* **2019**, *71*, 1–25. Available online: http://eadnurt.diit.edu.ua/jspui/handle/123456789/11681 (accessed on 21 December 2022).
22. Huang, H.; Li, K.; Wang, Y. A Simulation Method for Analyzing and Evaluating Rail System Performance Based on Speed Profile. *J. Syst. Sci. Syst. Eng.* **2018**, *27*, 810–834. [CrossRef]
23. De Martinis, V.; Weidmann, U.A. Definition of Energy-Efficient Speed Profiles Within Rail Traffic by Means of Supply Design Models. *Res. Transp. Econ.* **2015**, *54*, 41–50. [CrossRef]

24. Yang, Z.; Zhou, X.; Yao, F.; Wang, F.; Sun, C. Mechanism-Based Modeling and Estimation of Optimal Energy Consumption in Traffic Flow for Electric Vehicles. In Proceedings of the 2021 33rd Chinese Control and Decision Conference (CCDC), Kunming, China, 22–24 May 2021; pp. 1896–1903. [CrossRef]
25. Tian, Z.; Hillmansen, S.; Roberts, C.; Weston, P.; Chen, L.; Zhao, N.; Su, S.; Xin, T. Modeling and Simulation of DC Rail Traction Systems for Energy Saving. In Proceedings of the 17th International IEEE Conference on Intelligent Transportation Systems (ITSC), Qingdao, China, 8–11 October 2014; pp. 2354–2359. [CrossRef]
26. Fafoutellis, P.; Mantouka, E.G.; Vlahogianni, E.I. Eco-Driving and Its Impacts on Fuel Efficiency: An Overview of Technologies and Data-Driven Methods. *Sustainability* **2021**, *13*, 226. [CrossRef]
27. Das, K.; Borah, C.K.; Agarwal, S.; Barman, P.; Sharma, S. Road Load Model Analysis for Eco-Routing Navigation Systems in Electric Vehicles. In Proceedings of the 2019 IEEE 89th Vehicular Technology Conference (VTC2019-Spring), Kuala Lumpur, Malaysia, 28 April–1 May 2019; pp. 1–5. [CrossRef]
28. Feng, X.; Zhang, H.; Ding, Y.; Liu, Z.; Peng, H.; Xu, B. A Review Study on Traction Energy Saving of Rail Transport. *Discret. Dyn. Nat. Soc.* **2013**, *2013*, 156548. [CrossRef]
29. Wang, Y.Z.; Zhou, S.; Ou, X.M. Development and Application of a Life Cycle Energy Consumption and CO_2 Emissions Analysis Model for High-Speed Railway Transport in China. *Adv. Clim. Chang. Res.* **2021**, *12*, 270–280. [CrossRef]
30. Guevara-Cedeño, J.; Aguilar, J.; Torabi, R.; Berbey-Alvarez, A. Electric Mobility in Panama: A Review. In Proceedings of the 2018 Energy and Sustainability for Small Developing Economies (ES2DE), Funchal, Portugal, 9–12 July 2018; pp. 1–6. [CrossRef]
31. Thiel, C.; Amillo, A.G.; Tansini, A.; Tsakalidis, A.; Fontaras, G.; Dunlop, E.; Taylor, N.; Waldau-Jäger, A.; Araki, K.; Nishioka, K.; et al. Impact of Climatic Conditions on Prospects for Integrated Photovoltaics in Electric Vehicles. *Renew. Sustain. Energy Rev.* **2022**, *158*, 112109. [CrossRef]
32. Benatia, D. Ring the Alarm! Electricity Markets, Renewables, and the Pandemic. *Energy Econ.* **2022**, *106*, 105755. [CrossRef]
33. Sun, Y.; Anwar, A.; Razzaq, A.; Liang, X.; Siddique, M. Asymmetric Role of Renewable Energy, Green Innovation, and Globalization in Deriving Environmental Sustainability: Evidence from Top-10 Polluted Countries. *Renew. Energy* **2022**, *185*, 280–290. [CrossRef]
34. Zhao, N.; Tian, Z.; Hillmansen, S.; Chen, L.; Roberts, C.; Gao, S. Timetable Optimization and Trial Test for Regenerative Braking Energy Utilization in Rapid Transit Systems. *Energies* **2022**, *15*, 4879. [CrossRef]
35. Berbey, A.; Galán, R.; San Segundo, P.; Sanz-Bobi, J. Lyapunov Based Stability Analysis for Metro Lines. In *Urban Transport XIV: Urban Transport and the Environment in the 21st Century*; WIT Press: Southampton, UK; Boston, MA, USA, 2008; pp. 111–119. [CrossRef]
36. Berbey, A.; Galán, R.; San Segundo, P.; Sanz Bobi, J.D.; y Caballero, R. Un Algoritmo de Replanificación en Tiempo Real Basado en un Indice de Estabilidad de Lyapunov Para Líneas de Metro. *Rev. Iberoam. Automática E Inf. Ind.* **2014**, *11*, 167–178. [CrossRef]
37. Zhou, L.; Tong, L.C.; Chen, J.; Tang, J.; Zhou, X. Joint Optimization of High-Speed Train Timetables and Speed Profiles: A Unified Modeling Approach Using Space-Time-Speed Grid Networks. *Transp. Res. Part B Methodol.* **2017**, *97*, 157–181. [CrossRef]
38. Wang, Y.; Zhu, S.; D'Ariano, A.; Yin, J.; Miao, J.; Meng, L. Energy-Efficient Timetabling and Rolling Stock Circulation Planning Based on Automatic Train Operation Levels for Metro Lines. *Transp. Res. Part C Emerg. Technol.* **2021**, *129*, 103209. [CrossRef]
39. Songpo, Y.; Jianjun, W.; Xin, Y.; Huijun, S.; Ziyou, G. Energy-Efficient Timetable and Speed Profile Optimization with Multi-Phase Speed Limits: Theoretical Analysis and Application. *Appl. Math. Model.* **2018**, *56*, 32–50. [CrossRef]
40. Wilk, A.; Gelman, L.; Skibicki, J.; Judek, S.; Karwowski, K.; Jakubowski, A.; Kaczmarek, P. Novel Vision Monitoring Method Based on Multi Light Points for Space-Time Analysis of Overhead Contact Line Displacements. *Sensors* **2022**, *22*, 9281. [CrossRef] [PubMed]
41. Leung, C.M.; Or, S.W.; Ho, S.L.; Lee, K.Y. Wireless Condition Monitoring of Train Traction Systems Using Magnetoelectric Passive Current Sensors. *IEEE Sens. J.* **2014**, *14*, 4305–4314. [CrossRef]
42. Danielsen, S.; Fosso, O.B.; Molinas, M.; Suul, J.A.; Toftevaag, T. Simplified Models of a Single-Phase Power Electronic Inverter for Railway Power System Stability Analysis—Development and Evaluation. *Electr. Power Syst. Res.* **2010**, *80*, 204–214. [CrossRef]
43. Biliński, J.; Malczewska, M.; Rojek, A.; Kruczek, W. Static Converters of Railway Vehicles—Technical Solutions and Directions of Construction Development. *TTS Tech. Transp. Szyn.* **2020**, *27*, 43–57.
44. Biliński, J.; Łagosz, M. Metodology for Determination of the a Heart Losses and Thermal Loads in Traction Invertes. *TTS Tech. Transp. Szyn.* **2016**, *23*, 24–27.
45. Zhong, Q.C.; Hornik, T. *Control of Power Inverters in Renewable Energy and Smart Grid Integration*, 1st ed.; John Wiley & Sons: London, UK, 2013.
46. Hulagu, S.; Celikoglu, H.B. Electric Vehicle Location Routing Problem with Vehicle Motion Dynamics-Based Energy Consumption and Recovery. *IEEE Trans. Intell. Transp. Syst.* **2021**, *23*, 10275–10286. [CrossRef]
47. Evans, J.; Berg, M. Challenges in Simulation of Rail Vehicle Dynamics. *Veh. Syst. Dyn.* **2009**, *47*, 1023–1048. [CrossRef]
48. Bondarenko, I.; Severino, A.; Olayode, I.O.; Campisi, T.; Neduzha, L. Dynamic Sustainable Processes Simulation to Study Transport Object Efficiency. *Infrastructures* **2022**, *7*, 124. [CrossRef]
49. Myamlin, S.; Neduzha, L.; Ten, O.; Shvets, A. Determination of Dynamic Performance of Freight Cars Taking Into Account Technical Condition of Side Bearers. *Sci. Transp. Prog.* **2013**, *1*, 162–169. [CrossRef] [PubMed]
50. Cheli, F.; Di Gialleonardo, E.; Melzi, S. Freight Trains Dynamics: Effect of Payload and Braking Power Distribution on Coupling Forces. *Veh. Syst. Dyn.* **2017**, *55*, 464–479. [CrossRef]

51. Kovalchuk, V.; Sysyn, M.; Gerber, U.; Nabochenko, O.; Zarour, J.; Dehne, S. Experimental Investigation of the Influence of Train Velocity and Travel Direction on the Dynamic Behavior of Stiff Common Crossings. *Facta Univ. Ser. Mech. Eng.* **2019**, *17*, 345–356. [CrossRef]
52. Jóvér, V.; Gáspár, L.; Fischer, S. Investigation of Tramway Line No. 1, in Budapest, Based on Dynamic Measurements. *Acta Polytech. Hung.* **2022**, *19*, 65–76. [CrossRef]
53. Li, X.; Lo, H.K. Energy Minimization in Dynamic Train Scheduling and Control for Metro Rail Operations. *Transp. Res. Part B Methodol.* **2014**, *70*, 269–284. [CrossRef]
54. Gonzalez, R.; Jayakumar, P.; Iagnemma, K. Generation of Stochastic Mobility Maps for Large-Scale Route Planning of Ground Vehicles: A Case Study. *J. Terramechanics* **2017**, *69*, 1–11. [CrossRef]
55. Zhong, W.; Li, S.; Xu, H.; Zhang, W. On-line Train Speed Profile Generation of High-Speed Railway with Energy-Saving: A Model Predictive Control Method. *IEEE Trans. Intell. Transp. Syst.* **2020**, *23*, 4063–4074. [CrossRef]
56. Bin, Z.; Shijun, Y.; Lanfang, Z.; Daming, L.; Yalan, C. Energy-Efficient Speed Profile Optimization for High-Speed Railway Considering Neutral Sections. *IEEE Access* **2021**, *9*, 25090–25100. [CrossRef]
57. Heirich, O.; Robertson, P.; Strang, T. RailSLAM-Localization of Rail Vehicles and Mapping of Geometric Railway Tracks. In Proceedings of the 2013 IEEE International Conference on Robotics and Automation, Karlsruhe, Germany, 6–10 May 2013; pp. 5212–5219. [CrossRef]
58. Lei, X.; Noda, N.A. Analyses of Dynamic Response of Vehicle and Track Coupling System with Random Irregularity of Track Vertical Profile. *J. Sound Vib.* **2002**, *258*, 147–165. [CrossRef]
59. Burak-Romanowski, R.; Woźniak, K. Energy Aspects of Modernization of Railway Lines. *Tech. Trans. Electrtical Eng.* **2011**, *108*, 13–29.
60. Kacprzak, J. *Teoria Trakcji Elektrycznej*; Wydawnictwo Politechniki Warszawskiej: Warszawa, Poland, 1996.
61. Biliński, J.; Błażejewski, M.; Malczewska, M.; Szczepiórkowska, M. Resistance of Traction Vehicles Movement—Empirical Equations (1). *TTS Tech. Transp. Szyn.* **2019**, *26*, 34–39.
62. Kampczyk, A. Determinants of Specific Traction Electricity Consumption in a Sustainability Development System Rail Transport. In Proceedings of the International Scientific Conference Innovations 4.0 in the Post COVID Global World, (ISCIW 2022), Warsaw, Poland, 4–6 October 2022.
63. Kampczyk, A.; Gamon, W.; Gawlak, K. Implementation of Non-Contact Temperature Distribution Monitoring Solutions for Railway Vehicles in a Sustainability Development System Transport. *Sensors* **2022**, *22*, 9624. [CrossRef]
64. Geoportal for Spatial Information Infrastructure. Geoportal Infrastruktury Informacji Przestrzennej. Available online: https://mapy.geoportal.gov.pl/imap/Imgp_2.html (accessed on 4 January 2023).
65. Technical Conditions for Maintaining Track Surface on Railway Lines Id-1 (D-1). Warsaw. 2015. Available online: https://www.plk-sa.pl/klienci-i-kontrahenci/akty-prawne-i-przepisy/instrukcje-pkp-polskich-linii-kolejowych-sa/linie-kolejowe (accessed on 21 January 2023).
66. Regulation of the Minister of Transport and Maritime Economy of 10 September 1998 on Technical Conditions to Be Met by Railway Structures and Their Location. Available online: http://isap.sejm.gov.pl/isap.nsf/DocDetails.xsp?id=WDU19981510987 (accessed on 24 January 2023).
67. Act of 28 March 2003 on Railway Transport. Available online: https://isap.sejm.gov.pl/isap.nsf/DocDetails.xsp?id=wdu20030860789 (accessed on 24 January 2023).
68. Act of 7 July 1994. Building Law. Available online: https://isap.sejm.gov.pl/isap.nsf/DocDetails.xsp?id=wdu19940890414 (accessed on 24 January 2023).
69. Act of 17 May 1989. Geodetic and Cartographic Law. Available online: https://isap.sejm.gov.pl/isap.nsf/DocDetails.xsp?id=WDU19890300163 (accessed on 9 January 2023).
70. *Technical Conditions for Maintaining Track Surface on Railway Lines Id-1 (D-1)*; PKP Polskie Linie Kolejowe: Warsaw, Poland, 2005.
71. 4 Types of Classification of Terrain. Available online: https://civilnoteppt.com/4-types-of-classification-of-terrain-highway-engineering/ (accessed on 9 December 2022).
72. Prinz, D.; Oweis, T.; Oberle, A. Rainwater Harvesting for Dry Land Agriculture—Developing a Methodology Based on Remote Sensing and GIS. In Proceedings of the XIII International Congress of Agricultural Engineering, Rabat, Morocco, 2–6 February 1998.
73. Encyklopedia Leśna. Równina. Available online: https://www.encyklopedialesna.pl/haslo/rownina-1/ (accessed on 7 December 2022).
74. Klimaszewski, M. *Geomorfologia Polski, t. 1 i 2*; PWN: Warszawa, Poland, 1994.
75. Starkel, L. *Geografia Polski—Środowisko Przyrodnicze*; PWN: Warszawa, Poland, 1999.
76. Regulation of the Council of Ministers of 15 October 2012 on the National Spatial Reference System. Available online: https://isap.sejm.gov.pl/isap.nsf/DocDetails.xsp?id=WDU20120001247 (accessed on 21 December 2022).
77. Technical Standard Specifying the Principles and Accuracy of Surveying Measurements for the Installation of Multifunctional Railway Track Axis Adjustment Signs Ig-7. 2018. Available online: https://www.plk-sa.pl/klienci-i-kontrahenci/akty-prawne-i-przepisy/geodezja (accessed on 14 December 2022).
78. Technical Standard About Organization and Execution of Measurements in Railway Surveying GK-1, Warsaw. 2015. Available online: https://www.pkp.pl/pl/geodezja-i-kartografia/informacje-ogolne (accessed on 17 December 2022).

79. Regulation of the Minister of Development of 18 August 2020 on the Technical Standards for Performing Situational and Elevation Geodetic Measurements and for Developing and Transferring the Results of Such Measurements to the National Geodetic and Cartographic Resource. Available online: https://isap.sejm.gov.pl/isap.nsf/DocDetails.xsp?id=WDU20200001429 (accessed on 17 January 2023).
80. *PN-EN 50463*; Railway Applications—Measurement of Energy on Board a Train. PKN: Warsaw, Poland, 2020.
81. Scheepmaker, G.M.; Willeboordse, H.Y.; Hoogenraad, J.H.; Luijt, R.S.; Goverde, R.M.P. Comparing Train Driving Strategies on Multiple Key Performance Indicators. *J. Rail Transp. Plan. Manag.* **2020**, *13*, 100163. [CrossRef]
82. Kuźmiński, Ł.; Maśloch, P.; Bazan, M.; Janiczek, T.; Halawa, K.; Wojtaszek, H.; Miciuła, I.; Chajduga, T.; Kawecki, A.; Czwartosz, R.; et al. Management of Delay Optimization at Intersections. *Energies* **2020**, *13*, 3087. [CrossRef]
83. Wojtaszek, H.; Miciuła, I. Analysis of Factors Giving the Opportunity for Implementation of Innovations on the Example of Manufacturing Enterprises in the Silesian Province. *Sustainability* **2019**, *11*, 5850. [CrossRef]
84. Żywiołek, J.; Rosak-Szyrocka, J.; Mrowiec, M. Knowledge Management in Households about Energy Saving as Part of the Awareness of Sustainable Development. *Energies* **2021**, *14*, 8207. [CrossRef]
85. Ibrahim, A.; Jiang, F. The Electric Vehicle Energy Management: An Overview of the Energy System and Related Modeling and Simulation. *Renew. Sustain. Energy Rev.* **2021**, *144*, 111049. [CrossRef]
86. Maciuk, K. Monitoring of Galileo on-Board Oscillators Variations, Disturbances & Noises. *Measurement* **2019**, *147*, 106843. [CrossRef]
87. Maciuk, K. GPS-only, GLONASS-only and Combined GPS+GLONASS Absolute Positioning under Different Sky View Conditions. *Teh. Vjesn.* **2018**, *25*, 933–939. [CrossRef]
88. Jánešová, M.; Kratochvíl, R. Use of Clustering for Creating Economic-Mathematical Model of Aweb Portal. *Neural Netw. World* **2019**, *2*, 61–70. [CrossRef]
89. González-Gil, A.; Palacin, R.; Batty, P. Sustainable Urban Rail Systems: Strategies and Technologies for Optimal Management of Regenerative Braking Energy. *Energy Convers. Manag.* **2013**, *75*, 374–388. [CrossRef]

Disclaimer/Publisher's Note: The statements, opinions and data contained in all publications are solely those of the individual author(s) and contributor(s) and not of MDPI and/or the editor(s). MDPI and/or the editor(s) disclaim responsibility for any injury to people or property resulting from any ideas, methods, instructions or products referred to in the content.